Cocrystallization Behavior of Poly(butylene terephthalate-*co*-butylene 2,6-naphthalate) Random Copolymers

Young Gyu Jeong and Won Ho Jo*

Hyperstructured Organic Materials Research Center and Department of Fiber and Polymer Science, Seoul National University, Seoul 151-742, Korea

Sang Cheol Lee

Department of Polymer Science and Engineering, Kumoh National University of Technology, Kumi 730-701, Korea

Received January 11, 2000; Revised Manuscript Received October 13, 2000

ABSTRACT: A series of poly(butylene terephthalate-*co*-butylene 2,6-naphthalate) (P(BT-*co*-BN)) random copolymers were synthesized, and their cocrystallization behavior was investigated by differential scanning calorimetry (DSC) and wide-angle X-ray diffraction (WAXD). The P(BT-*co*-BN) copolymers, which are found to be statistical random copolymers, show a single melting and a single crystallization peak over the entire range of copolymer composition and have a eutectic melting point in the plot of melting point versus composition. WAXD patterns of copolymers are divided into two groups, i.e., the PBT type crystal and the PBN type crystal. These facts indicate that the P(BT-*co*-BN) copolymers show isodimorphic cocrystallization. The eutectic composition at which the crystal transition between PBT and PBN type crystal occurs was estimated ca. 35 mol % BN content. When the defect free energy was calculated by using the equilibrium inclusion model, the defect free energy (6.10 kJ/mol) in the case of incorporation of BN units in the PBT type crystal was higher than the opposite case (3.63 kJ/mol). It means that the incorporation of bulkier BN units in the PBT type crystal is more sterically hindered than the opposite case. The changes of heat of fusion and *d* spacings with composition also support isodimorphic crystallization.

Introduction

Poly(butylene terephthalate) (PBT) has been widely used for an engineering thermoplastic or for a component in blends[1−5] and copolymers.[5,6] It has many applications such as molding and fiber spinning because of its fast crystallization rate and high elasticity compared to those of poly(ethylene terephthalate) while exhibiting desirable physical and mechanical properties. Early research has discovered that PBT exists in two crystalline structures, α and *β* forms, and that the transition between two forms takes place reversibly by mechanical deformation, i.e., the transition from α form to *β* form takes place by elongation and vice versa by relaxation.[7−9]

Poly(butylene 2,6-naphthalate) (PBN) has recently attracted much interest from industry, since it has many useful properties such as gas barrier property and thermostability. As can be seen in Figure 1, the chemical structure of PBN is equivalent to that of PBT except that only the benzene ring is replaced by the naphthalene ring. It has recently been found that PBN also has two crystal forms, A and B forms, and that four methylene groups in the B form is more extended than that of the A form as in the case of PBT.[10,11] Under the absence of mechanical deformation, both the crystal structures of PBT and PBN favor the α form and A form, respectively. As can be seen in Table 1, the unit cell parameters, *a* and *b*, of PBT α form and PBN A form are almost the same while the unit cell parameter, *c*, of PBT α form is somewhat different from that of PBN A form. This leads us to expect that cocrystallization between PBT and PBN units may occur in the crystalline phase of PBT/PBN copolymers.

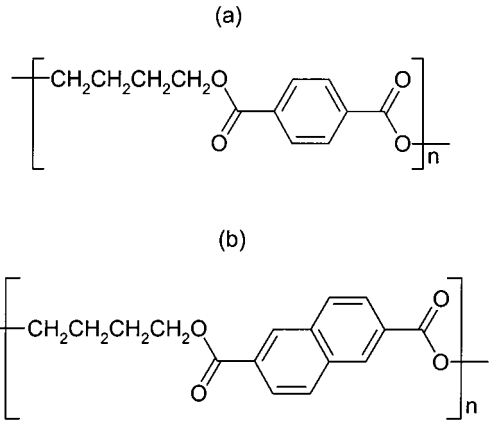

Figure 1. Chemical structures of PBT (a) and PBN (b).

Cocrystallization behavior in copolymers whose component homopolymers are both crystalline is a rare phenomenon. Only a few systems including poly(3-hydroxybutyrate-*co*-3-hydroxyvalerate) (P(3HB-*co*-3HV)) copolymers[12−19] have been reported to show cocrystallization which is manifested by the presence of a clear melting temperature over the entire range of composition.

Cocrystallization is divided into two groups, i.e., isomorphism and isodimorphism. When two components have the similar chemical structure and thus occupy approximately the same volume, the excess free energy of cocrystallizaion would be very small, and therefore the chain conformation of both corresponding homopolymers becomes compatible with either crystal lattice, so-

* To whom correspondence should be addressed. Tel 82-2-880-7192; Fax 82-2-885-1748; E-mail whjpoly@plaza.snu.ac.kr.

10.1021/ma000040n CCC: $19.00
Published on Web 12/02/2000

Table 1. Crystallographic Data for PBT and PBN

	PBT[9]		PBN[10,11]	
	α-form	β-form	A-form	B-form
crystal system	triclinic	triclinic	triclinic	triclinic
space group	$P\bar{1}$	$P\bar{1}$	$P\bar{1}$	$P\bar{1}$
cell parameters				
a (nm)	0.483	0.495	0.487	0.455
b (nm)	0.594	0.567	0.622	0.643
c (nm)	1.159	1.295	1.436	1.531
α (deg)	99.7	101.7	100.8	110.1
β (deg)	115.2	121.8	126.9	121.1
γ (deg)	110.8	99.9	97.9	100.6
conformation of the 4 methylene groups	$\bar{G}\bar{G}TGG$	$TST\bar{S}T$	$\bar{S}\bar{G}TGS$	$TST\bar{S}T$
repeating units/unit cell	1	1	1	1
density (g/cm^3)	1.40	1.28	1.36	1.39

called isomorphism.[20] As a result, only one crystalline phase containing both comonomer units is detected at all compositions. On the other hand, copolymers may show isodimorphism where two crystalline phases, each of which contains comonomer units as a minor component, are observed. In this case, an increase in the content of the minor component in each crystalline phase is accompanied by a lowering of the melting and crystallization temperatures. In this case, a melting point minimum is observed in the plot of melting point versus copolymer composition.

In this study, PBT, PBN, and poly(butylene terephthalate-*co*-butylene 2,6-naphthalate) (P(BT-*co*-BN)) random copolymers were synthesized and characterized by ^{1}H NMR spectroscopy and viscometry, and the cocrystallization behavior of P(BT-*co*-BN) was investigated by using differential scanning calorimetry (DSC) and wide-angle X-ray diffraction (WAXD). The cocrystallization behavior was also analyzed thermodynamically by the equilibrium inclusion model proposed by Wendling and Suter,[21] from which the average defect free energy was estimated.

Experimental Section

Materials. PBT, PBN, and P(BT-*co*-BN) copolymers used in this study were prepared from dimethyl terephthalate (DMT), dimethyl-2,6-naphthalate (DMN), and 1,4-butanediol (BD) using titanium tetrabutoxide as a catalyst. The two-step polymerization was performed on a laboratory-scale polymerization reactor in the molten state. The first step was the transesterification reaction of DMT and DMN with BD, and the second was the polycondensation reaction. The monomers and catalyst were mixed in a glass-made reaction vessel, and the mixture was gradually heated under constant stirring. The transesterification reaction was carried out at 190 °C under nitrogen atmosphere, and the reaction was controlled by the amount of the distilled methanol. The polycondensation was carried out at 260 °C under high-vacuum conditions. At the end of the reaction, the products in the melt were quenched into water bath and followed by drying in a vacuum oven. The monomer composition in the feed was varied from 0, 10, 30, 50, 70, 90, to 100 wt % of BN. The polymers synthesized were purified by the solution/precipitation method. The polymers were first dissolved in a mixed solvent of phenol/1,1,2,2-tetrachloroethane (6/4, v/v), and subsequently the polymer solutions were poured into a large excess acetone. The precipitates were filtered, washed with excess acetone several times in order to extract residual solvent, and then dried in a vacuum oven at 40 °C for several days.

Characterization. The intrinsic viscosities of all samples in the mixture of phenol/1,1,2,2-tetrachloroethane (6/4, v/v) were measured on Ubbelohde viscometer at 35 °C. ^{1}H NMR spectroscopy was used for determining both the copolymer composition and the dyad sequence distribution in the copolymers. The ^{1}H NMR spectra of $CDCl_3/CF_3COOD$ solutions were recorded on a Bruker AMX500 operating at 500 MHz. On determination of the dyad sequence distribution, the relative peak intensities for BT/BT, BT/BN, and BN/BN dyads are deconvoluted, and their peak areas are considered to be corresponding dyad quantities.

Thermal Analysis and Crystallization Kinetics. The thermal and crystallization properties of the samples were measured with a Perkin-Elmer DSC-7 differential scanning calorimeter equipped with an intercooler system. The DSC was calibrated with high-purity indium standard (156.6 °C and 28.45 J/g) for melting temperature and heat of fusion. PBT, PBN, and P(BT-*co*-BN) samples were compression-molded into thin films in a hot plate at 280 °C for 5 min and quenched in liquid nitrogen. Relatively small sample sizes (5 ± 0.3 mg) were used to minimize the effect of thermal conductivity of polymers. Unless otherwise specified, the heating rate and the cooling rate were 20 and 10 °C/min, respectively. All scans were carried out under a nitrogen atmosphere to minimize the oxidative degradation. The peak temperatures of melting of quenched samples are taken as the apparent melting temperatures.

The isothermal crystallization study was examined by monitoring the heat flow of crystallization on DSC as a function of time. The copolymer samples were heated to the temperature 20 °C higher than their respective melting temperatures, held for 5 min in order to completely melt the crystal, and then rapidly cooled to the predetermined crystallization temperature (T_c). The inverse ($t_{1/2}^{-1}$) of the time required to attain 50% overall crystallization was used as a measure of the overall crystallization rate. The equilibrium melting temperatures (T_m^o) of the samples are obtained from the Hoffman−Weeks plots.[22] The dynamic crystallization experiments were performed by varying the cooling rate with 10, 20, 40, 80, and 160 °C/min, to examine the effect of cooling rate on crystallization behavior of the samples from the melt.

WAXD Analysis. The diffraction pattern was obtained on a MAC Science M18XHF X-ray diffractometer using Ni-filtered Cu−Kα radiation ($\lambda = 0.1542$ nm, 50 V, 100 mA) at a scanning rate of 5°/min. The diffractometer was equipped with a $\theta-2\theta$ goniometer, a divergence slit (1.0°), a scattering slit (1.0°), and a receiving slit (0.30 mm). Si powder as a standard was run for the angular calibration under the same condition. The samples for WAXD were prepared in film forms. All samples were compression-molded into the films using a hot press at the temperature 20 °C higher than their melting temperatures, cooled to the temperature 20 °C lower than their apparent melting temperatures, and then annealed for 2 h. The X-ray crystallinity was evaluated from the diffracted intensity data in the range of $2\theta = 5-40°$ according to the Ruland-Vonk's method[23,24] after the Lorentz and polarization factor correction. Amorphous contribution to the X-ray scattering was estimated from the WAXD patterns for quenched amorphous samples.

Results and Discussion

Synthesis and Characterization. A typical ^{1}H NMR spectrum of P(BT-*co*-BN) copolymer and the assignment of each peak are shown in Figure 2. The peaks corresponding to the protons in naphthalene ring of BN unit can be easily separated into two groups by magnetically different environment. The equation for determining the copolymer composition from respective peak area is given

$$\frac{c+d}{e} = \frac{a}{e} = \frac{b}{e} = \frac{2(X+Y)}{Y} \qquad (1)$$

where *a*, *b*, *c*, *d*, and *e* represent the areas of corresponding peaks in Figure 2, and *X* and *Y* denote the mole fractions of BT and BN units, respectively. When the copolymer compositions as calculated by eq 1 are compared with the feed composition, it is revealed that

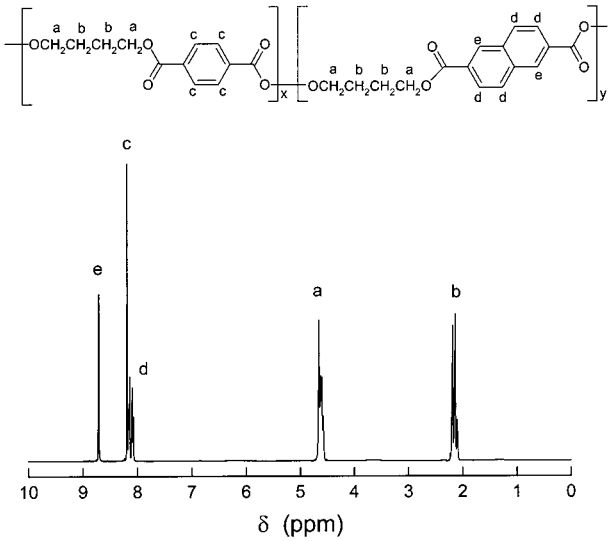

Figure 2. A typical ^{1}H NMR spectrum of P(BT-*co*-BN) copolymer and its peak assignment.

Table 2. Characteristics of the Synthesized Random Copolymers

sample code	feed composition (mol %) BT	feed composition (mol %) BN	copolymer composition[a] (mol %) BT	copolymer composition[a] (mol %) BN	intrinsic viscosity (dL/g)
PBN	0.0	100.0	0.0	100.0	0.69
P(BT-*co*-88 mol % BN)	12.3	87.7	11.9	88.1	0.75
P(BT-*co*-64 mol % BN)	35.0	65.0	35.7	64.3	0.77
P(BT-*co*-43 mol % BN)	55.7	44.3	56.8	43.2	0.84
P(BT-*co*-25 mol % BN)	74.5	25.5	76.5	24.5	0.87
P(BT-*co*-7 mol % BN)	91.9	8.1	92.7	7.3	0.77
PBT	100.0	0.0	100.0	0.0	0.79

[a] Measured by ^{1}H NMR.

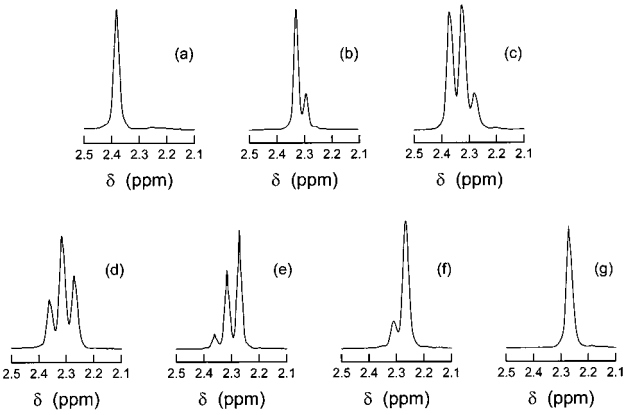

Figure 3. ^{1}H NMR spectra in the range of 2.1−2.5 ppm: (a) PBN; (b) P(BT-*co*-88 mol % BN); (c) P(BT-*co*-64 mol % BN); (d) P(BT-*co*-43 mol % BN); (e) P(BT-*co*-25 mol % BN); (f) P(BT-*co*-7 mol % BN); (g) PBT.

the copolymer compositions are nearly equal to the feed compositions, as can be seen from Table 2. The intrinsic viscosities of the samples are in the range of 0.69−0.87 dL/g, as shown in Table 2, indicating that the synthesized polymers have relatively high molecular weight enough to be formed in film.

The ^{1}H NMR spectra in the range of 2.1−2.5 ppm are shown in Figure 3, where three peaks are assigned to BT/BT (2.27 ppm), BT/BN (2.32 ppm), and BN/BN (2.37 ppm) dyads. The relative concentrations of the three dyads are determined from deconvoluted areas of the

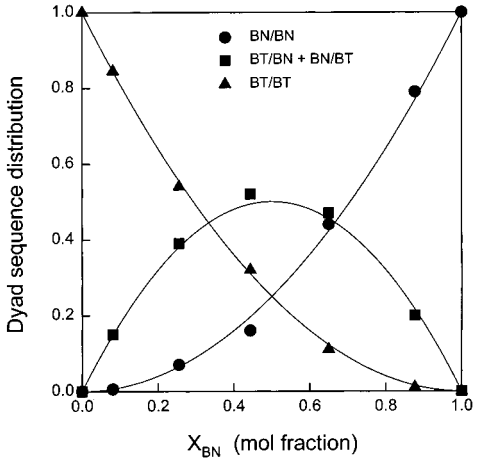

Figure 4. Dyad sequence distributions as a function of copolymer composition. The solid lines represent the calculated distribution based on the Bernoullian statistics.

three signals. In Figure 4, the dyad sequence distributions determined by ^{1}H NMR spectra are plotted against the mole fraction of BN composition. If the sequence distribution of a copolymer is statistically random, the dyad sequence distribution obeys the Bernoullian statistics:

$$P_{BT/BT} = P_{BT}^2$$
$$P_{BT/BN} = P_{BN/BT} = P_{BT}P_{BN}$$
$$P_{BN/BN} = P_{BN}^2 \qquad (2)$$

where $P_{i/j}$ and P_i denote the mole fractions of the *i*/*j* dyad sequence and *i* component in the copolymer chains, respectively. Since the fractions of dyad sequence determined experimentally are in good agreement with the dyad sequence distributions calculated by the Bernoullian statistics, as can be seen in Figure 4, it is concluded that the P(BT-*co*-BN) samples synthesized in this study are statistically random copolymers.

Thermal Property and Crystallization Kinetics. The heating and cooling thermograms of the quenched samples are shown in Figure 5. For all copolymer samples, a single melting and a single crystallization temperature are observed, which may be a strong evidence for cocrystallization. Furthermore, the change of the melting and crystallization temperatures with the BN composition exhibits a typical eutectic behavior, indicating that the copolymers show an isodimorphic cocrystallization. A closer examination of Figure 5B shows the broadening of the crystallization exotherms of the copolymers with 43 and 25 mol % BN represented by DSC thermograms (d) and (e). This broadening may arise from concurrent crystallization of two different crystals at the nearly same crystallization temperature. To resolve the broad peak into two peaks, the copolymer with 43 mol % BN was dynamically crystallized by varying the cooling rate. As can be seen in Figure 6, the exothermic peak position shifts to lower temperatures, concurrently with more distinct separation into two peaks, as the cooling rate is increased. This also supports the isodimorphic cocrystallization from two different crystals. The composition showing the lowest melting temperature corresponds to the transition point where the crystal transition between PBT and PBN crystal lattices occurs. This isodimorphic behavior is also

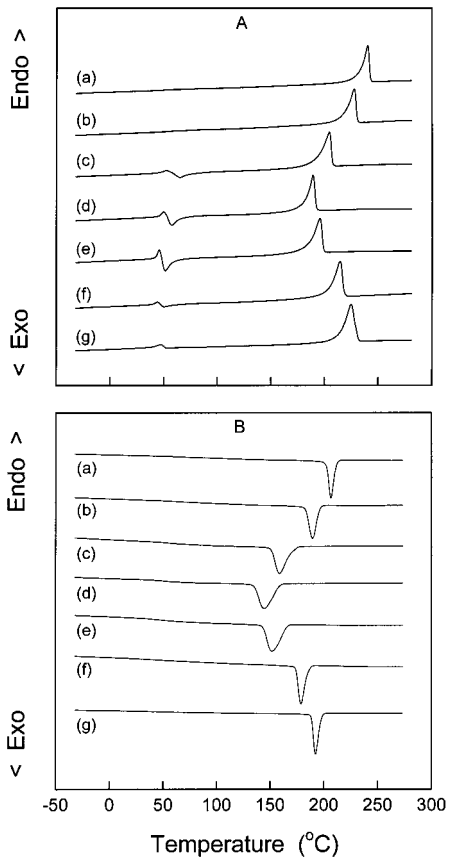

Figure 5. DSC heating (A) and cooling (B) thermograms for the quenched samples: (a) PBN; (b) P(BT-*co*-88 mol % BN); (c) P(BT-*co*-64 mol % BN); (d) P(BT-*co*-43 mol % BN); (e) P(BT-*co*-25 mol % BN); (f) P(BT-*co*-7 mol % BN); (g) PBT.

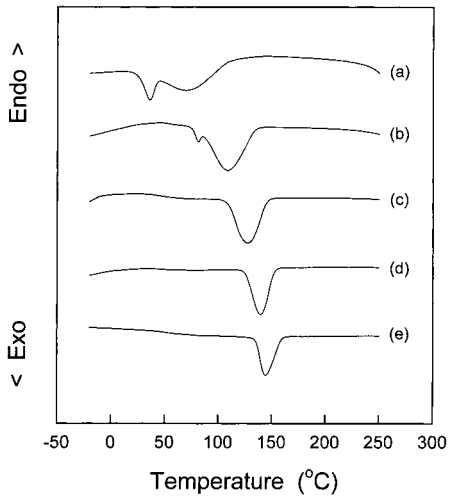

Figure 6. Dynamic crystallization for P(BT-*co*-43 mol % BN) at the various cooling rates: (a) 160, (b) 80, (c) 40, (d) 20, and (e) 10 °C/min.

observed in the relationship between the heat of fusion and the copolymer composition, as shown in Figure 7. In the cooling thermograms (Figure 5B), the crystallization temperature becomes lower as the comonomer composition is increased, indicating that the crystallization rate decreases with increasing the comonomer content due to an additional restriction of comonomer on the crystal lattice formation. This fact is confirmed by examining the plot of the inverse ($t_{1/2}^{-1}$) of crystallization half-time versus the degree of undercooling ($\Delta T = T_m^o - T_c$), as shown in Figure 8. At the same degree

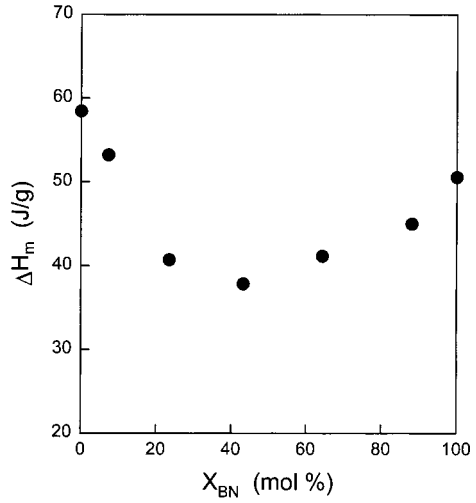

Figure 7. Heat of fusion as a function of copolymer composition.

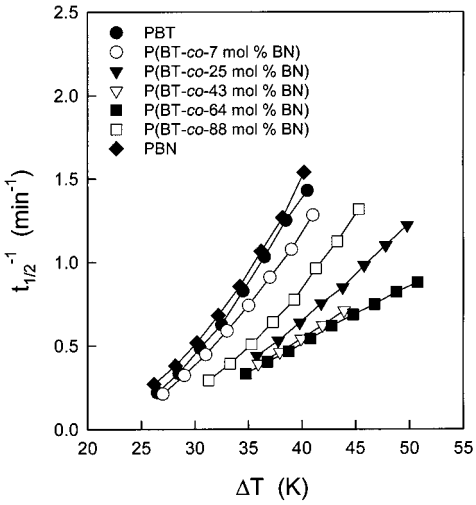

Figure 8. Inverse ($t_{1/2}^{-1}$) of crystallization half-time as a function of degree of undercooling.

of undercooling, for example ΔT = 37 °C, the overall crystallization rates of homopolymers are faster than those of copolymers. Figure 8 also shows that the overall crystallization rate of PBN is comparable with that of PBT homopolymer and that the copolymers show a pseudoeutectic behavior in the overall crystallizatiion rates. Scandola et al.[17] have reported that the P(3HB-*co*-3HV) copolymers also show pseudoeutectic behavior in the radial growth rate of spherulites.

The melting temperatures of the melt-crystallized samples are reported in Figure 9 as a function of the crystallization temperature. The data are well fitted by straight line; the intersections of these straight lines with the line $T_m = T_c$ give the equilibrium melting temperature (T_m^o) of the samples. The T_m^o of PBT and PBN homopolymers are approximately 506 and 520 K, respectively. The T_m^o of PBT is the same as the value reported by Pompe et al.[23]

WAXD Analysis. It has been known that the comonomer concentration in crystal lattice is strongly dependent on the copolymer composition in bulk and crystallization condition.[16,18] The extent of cocrystallization can qualitatively be measured by the change of the lattice *d* spacings in the WAXD patterns.[12b,18] In Figure 10, the reflections observed for PBT and PBN correspond to those of the PBT α form and PBN A form crystal,

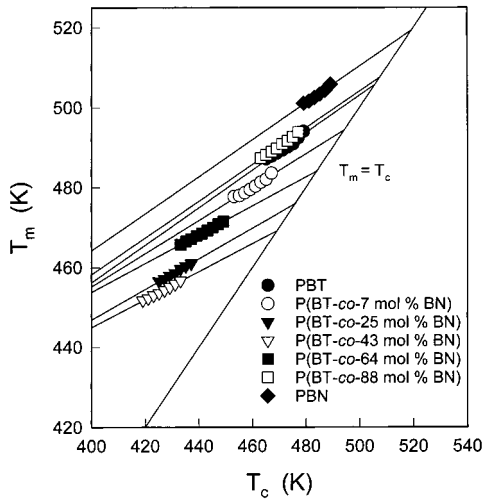

Figure 9. Hoffman−Weeks plots for obtaining the equilibrium melting temperatures of the melt-crystallized samples.

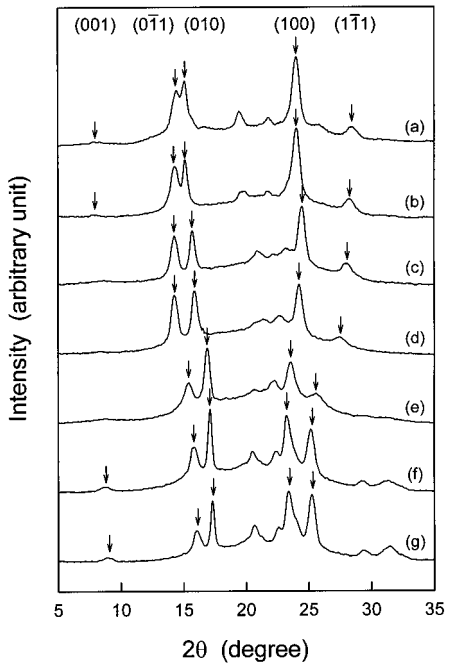

Figure 10. X-ray diffraction patterns of annealed samples: (a) PBN; (b) P(BT-*co*-88 mol % BN); (c) P(BT-*co*-64 mol % BN); (d) P(BT-*co*-43 mol % BN); (e) P(BT-*co*-25 mol % BN); (f) P(BT-*co*-7 mol % BN); (g) PBT.

respectively. The WAXD patterns in Figure 10 can be divided into two groups according to the BN content in the copolymer. The PBT type crystal structure develops up to 25 mol % BN content; i.e., the PBT lattice accommodates the BN units, whereas above 43 mol % BN the PBN type crystal structure develops. These WAXD patterns also support the isodimorphic cocrystallization of P(BT-*co*-BN) copolymers. Another point to be noted from Figure 10 is that X-ray diffractions of the (001) plane in respective PBT α type and PBN A type crystals are not discernibly observed for the samples with the composition of 25−43 mol %. This is because the amount of comonomer incorporated in the crystal lattice becomes larger with increasing the comonomer composition, and thereby the regularity in the direction along *c* axis becomes less than the lateral direction due to the considerable difference in the fiber period between PBT α type and PBN A type crystal. In agreement with

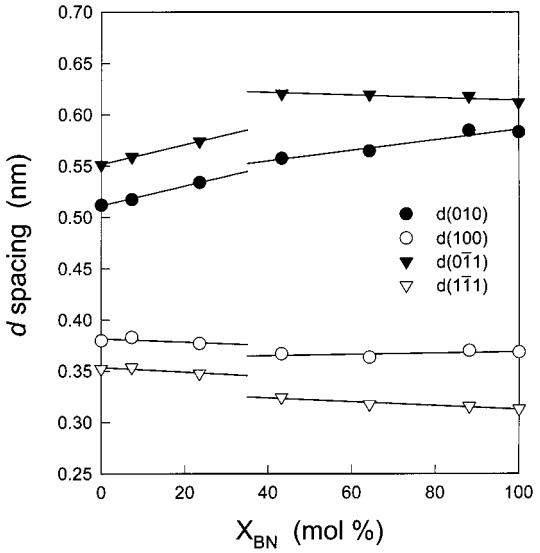

Figure 11. X-ray diffraction *d* spacings of the (010) and (100) planes for annealed samples as a function of copolymer composition.

the results of thermal analysis, the WAXD results also show that there exists the eutectic composition in the composition between 25 and 43 mol % BN units, where the crystalline phase changes from PBT α type to PBN A type crystal, as also can be seen in Figure 11.

As a consequence of comonomer inclusion, the *d* spacings of both crystal structures change with the comonomer content. As shown in Figure 11, in the PBT type crystal, the *d*(010) spacing gradually increases with increasing BN content, whereas the *d*(100) spacing slightly decreases. In the case of PBN type crystal, the *d*(010) spacing slightly decreases with increasing the BT content, while the *d*(100) spacing is almost constant irrespective of the BT content. The absence of any change of the *d*(100) spacing in PBN type crystal with composition can tentatively be explained by the fact that, in the PBN unit cell, the plane of naphthalene ring is aligned essentially along the (010) plane, and therefore the replacement of BN units with BT units does not perturb the crystal structure in the direction of [100]. When the increase of the *d*(100) spacing in PBT type crystal with composition is compared with the decrease of the *d*(100) spacing in PBN type crystal with composition, it is found that the expansion of PBT lattice by incorporation of BN units is larger than the contraction of PBN lattice by incorporation of BT units. This result suggests that the crystal lattice is more strongly perturbed when a larger comonomer is incorporated than does a smaller one.

Thermodynamics of Copolymer Crystallization. Several theories for copolymer crystallization have been developed, and the theories are largely classified into two types: the comonomer exclusion model[24,25] and the comonomer inclusion model.[15,26,27] Recently, Wendling and Suter[21] proposed a new model that combines the Sanchez−Eby model[27] (a comonomer inclusion model) with the Baur model[25] (a comonomer exclusion model). The model is given by

$$\frac{1}{T_m(X_B)} - \frac{1}{T_m^{\circ}} = \frac{R}{\Delta H_m^{\circ}}\left[\frac{\epsilon X_{CB}}{RT} + (1 - X_{CB}) \ln \frac{1 - X_{CB}}{1 - X_B} + X_{CB} \ln \frac{X_{CB}}{X_B} + \langle\tilde{\xi}\rangle^{-1}\right] \quad (3)$$

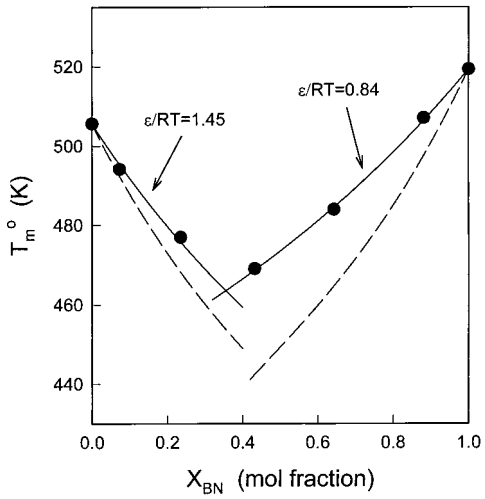

Figure 12. Comparison of the theoretical melting temperatures of P(BT-*co*-BN) with the equilibrium melting points experimentally determined. Dashed lines and solid lines represent the Baur model and the Wendling-Suter model, respectively.

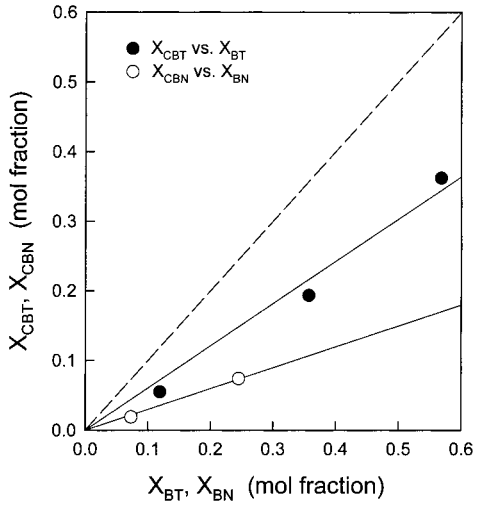

Figure 13. Equilibrium concentrations of BN and BT units incorporated in the respective PBT and PBN type crystal as a function of copolymer composition. The dashed line is based on the uniform inclusion model, and the solid lines are based on the linear regression.

where T_m^o and ΔH_m^o denote the homopolymer equilibrium melting temperature and the heat of fusion, respectively, R the gas constant, X_B the bulk composition of B units in the copolymer, X_{CB} the concentration of B units in the cocrystal, ϵ the average defect free energy, and $\langle\tilde{\xi}\rangle$ the average length sequence of homopolymer.

In the equilibrium comonomer inclusion, the concentration of B units in the cocrystal is given by[26,27]

$$X_{CB}^{eq} = \frac{X_B e^{-\epsilon/RT}}{1 - X_B + X_B e^{-\epsilon/RT}} \quad (4)$$

When X_{eq} in eq 3 is substituted by eq 4, eq 3 is simplified to the following equilibrium inclusion model:

$$\frac{1}{T_m^o} - \frac{1}{T_m(X_B)} = \frac{R}{\Delta H_m^o}[\ln(1 - X_B + X_B e^{-\epsilon/RT}) - \langle\tilde{\xi}\rangle^{-1}] \quad (5)$$

$$\langle\tilde{\xi}\rangle^{-1} = 2(X_B - X_B e^{-\epsilon/RT})(1 - X_B + X_B e^{-\epsilon/RT}) \quad (6)$$

When $X_{CB} = X_B$ and $X_{CB} = 0$, eq 3 reduces to the uniform inclusion model and the exclusion model, respectively.

In this study, the equilibrium inclusion model modified by Wendling and Suter was employed to determine the average defect free energy by comparing theoretical melting temperatures with equilibrium melting temperatures of P(BT-*co*-BN) random copolymers. The heat of fusion of PBT and PBN is 31[11,23] and 33 kJ/mol,[28] respectively. Figure 12 shows the comparison of the Wendling−Suter equilibrium inclusion model with experimental data of P(BT-*co*-BN) random copolymers, from which the ϵ/RT value is determined as an adjustable parameter. The model gives the constant ϵ/RT value regardless of the comonomer composition in both cases of PBT and PBN type crystal. When the average defect free energies were calculated from the values of ϵ/RT_m^o for PBT ($X_{BN} = 0$) and PBN ($X_{BT} = 0$), respectively, it is revealed that the average defect free energy (6.10 kJ/mol) in the case of incorporation of BN unit into the PBT type crystal is higher than the case of incorporation BT unit into the PBN crystal (3.63 kJ/mol). This indicates that a bulkier BN unit is more difficult to be included in PBT type crystal than the opposite case. The eutectic composition is estimated to be ca. 35 mol % BN from the intersection of the two melting temperature curves.

By use of eq 4 with the aid of the defect free energies determined from the above, equilibrium concentrations (X_{CB}) of comonomer units in the crystals are estimated. When X_{CB} is plotted against X_B, as shown in Figure 13, it is revealed that, in respective PBT and PBN crystal structure, the comonomer concentration in cocrystals increases with increasing the comonomer composition in bulk. However, in both cases, the comonomer concentration in each crystal is lower than the copolymer concentration in uniform inclusion model ($X_{CB} = X_B$). The equilibrium concentration of BT units in the PBN type crystal is different from that of BN units in the PBT type crystal at a given comonomer concentration in bulk because of the different defect free energies. It is noteworthy that, in the case of PBN type crystal, the plot of comonomer concentration (X_{CBT}) in cocrystal versus comonomer composition (X_{BT}) in bulk is not linear. This is because it is easier to create the excess volume necessary for a comonomer unit in an already imperfect crystal lattice than to create it in a defect-free crystal lattice, as noted by VanderHart et al.[18]

Conclusions

A series of P(BT-*co*-BN) copolymers synthesized in this study were found to be statistically random from ^{1}H NMR analysis. Nevertheless, for all copolymer compositions, there exist a clear melting and crystallization peak, which is a strong evidence for cocrystallization. The existence of a minimum in the plot of melting temperature against copolymer composition indicates that the copolymers exhibit isodimorphic cocrystallization. This isodimorphic cocrystallization behavior can also be shown in the WAXD patterns representing the variation of *d* spacings with the comonomer composition. These WAXD patterns are clearly divided into two groups according to comonomer composition, the PBT type crystal and the PBN type crystal. It is also found that the crystal transition between PBT and PBN type crystals occurs in the

eutectic composition between 25 and 43 mol % BN. The defect free energies are calculated by comparing the experimental melting temperatures to the Wendling–Suter equilibrium inclusion model of the melting temperature. The average defect free energy in the case of incorporation of BN units into PBT crystal lattice is higher than the opposite case, indicating bulkier BN units are difficult to be included in PBT crystal lattice than the opposite case.

References and Notes

(1) Hage, E.; Hale, W.; Keskkula, H.; Paul, D. R. *Polymer* **1997**, *38*, 117.
(2) Apstolov, A. A.; Fakirov, S.; Sezen, B.; Bahar, I.; Kloczkowski, A. *Polymer* **1994**, *35*, 451.
(3) Okamoto, M.; Inoue, T. *Polymer* **1994**, *35*, 257.
(4) Montaudo, G.; Puglisi, C.; Samperi, F. *Macromolecules* **1998**, *31*, 650.
(5) Gallagher, K. P.; Zhang, X.; Runt, J. P.; Huynh-ba, G. *Macromolecules* **1993**, *26*, 588.
(6) Stribeck, N.; Sapundjieva, D.; Denchev, Z.; Apostolov, A. A.; Zachmann, H. G.; Stamm, M.; Fakirov, S. *Macromolecules* **1997**, *30*, 1329.
(7) Jakeways, R.; Smith, T.; Ward, I. M.; Wilding, M. A. *Polym. Lett.* **1976**, *14*, 41.
(8) Hall, I. H.; Pass, M. G. *Polymer* **1976**, *17*, 807.
(9) Yokouchi, M.; Sakakibara, Y.; Chatani, Y.; Tadokoro, H.; Tanaka, T.; Yoda, K. *Macromolecules* **1976**, *9*, 266.
(10) Watanabe, H. *Kobunshi Ronbunshu* **1976**, *33*, 299.
(11) Koyano, K.; Yamamoto, Y.; Saito, Y.; Yamanobe, T.; Komoto, Y. *Polymer* **1998**, *39*, 4385.
(12) (a) Bloembergen, S.; Holden, D. A.; Hamer, G. K.; Bluhm, T. L.; Marchessault, R. H. *Macromolecules* **1986**, *19*, 2865. (b) Bluhm, T. L.; Hamer, G. K.; Marchessault, R. H.; Fyfe, C. A.; Veregin, R. P. *Macromolecules* **1986**, *19*, 2871.
(13) Kunioka, M.; Tamaki, A.; Doi, Y. *Macromolecules* **1989**, *22*, 694.
(14) Bloembergen, S.; Holden, D. A.; Bluhm, T. L.; Hamer, G. K.; Marchessault, R. H. *Macromolecules* **1989**, *22*, 1663.
(15) Kamiya, N.; Sakurai, M.; Inoue, Y.; Chujo, R. *Macromolecules* **1991**, *24*, 3888.
(16) Orts, W. J.; Marchessult, R. J.; Bluhm, T. L. *Macromolecules* **1991**, *24*, 6435.
(17) Scandola, M.; Ceccorulli, G.; Pizzoli, M.; Gazzano, M. *Macromolecules* **1992**, *25*, 1405.
(18) VanderHart, D.; Orts, W. J.; Marchessault, R. H. *Macromolecules* **1995**, *28*, 6394.
(19) Barker, P. A.; Barham, P. J.; Martinez-Salazar, J. *Polymer* **1997**, *38*, 913.
(20) Allegra, G.; Bassi, I. W. *Adv. Polym. Sci.* **1969**, *6*, 549.
(21) Wendling, J.; Suter, U. W. *Macromolecules* **1998**, *31*, 2516.
(22) Hoffman, J. D.; Weeks, J. J. *J. Res. Natl. Bur. Stand.* **1962**, *66A*, 13.
(23) Pompe, G.; Häubler, L.; Winter, W. *J. Polym. Sci., Polym. Phys. Ed.* **1996**, *34*, 211.
(24) (a) Flory, P. J. *J. Chem. Phys.* **1947**, *15*, 684. (b) Flory, P. J. *Trans. Faraday Soc.* **1955**, *51*, 848.
(25) Baur, V. H. *Makromol. Chem.* **1966**, *98*, 297.
(26) Helfand, E.; Lauritzen, J. I. *Macromoelcules* **1973**, *6*, 631.
(27) Sanchez, I. C.; Eby, R. K. *Macromolecules* **1975**, *8*, 638.
(28) Van Krevelen, D. W. *Properties of Polymers*; Elsevier Science Publishers: New York, 1990.

MA000040N